

Accelerated superradiance and collective atomic recoil lasing with a two-frequency pump

Mary M. Cola, Luca Volpe, and Nicola Piovella

Dipartimento di Fisica, Università degli Studi di Milano and INFN Sezione di Milano, Via Celoria 16, Milano I-20133, Italy

(Received 29 July 2008; revised manuscript received 6 October 2008; published 15 January 2009)

We demonstrate that superradiance and collective atomic recoil lasing from cold atoms can be enhanced using a two-frequency pump with frequency difference twice the two-photon recoil frequency ω_r . In the good-cavity regime the atoms behave as a three-recoil-level system, collectively scattering a single-frequency radiation mode. In the bad-cavity regime, the superradiant cascade through the different recoil momentum states is strongly accelerated. The emitted radiation shows a discrete spectrum whose harmonics are separated by $2\omega_r$ and generated by transitions between adjacent momentum levels.

DOI: [10.1103/PhysRevA.79.013613](https://doi.org/10.1103/PhysRevA.79.013613)

PACS number(s): 03.75.-b, 42.50.Gy, 34.50.-s

I. INTRODUCTION

The recent realization of a Bose-Einstein condensate coupled with a quantized field mode in a high-finesse optical cavity [1,2] has opened the opportunity to investigate different dynamical behaviors of coherent matter in the strong-coupling regime, such as, for instance, cold atoms trapped in a double-well potential [3] or the quantum magnetic dynamics of polarized light in arrays of microcavities [4]. Moreover, collective effects are greatly enhanced when a cold gas of weakly interacting atoms couples with radiation inside an optical cavity [5]. A paradigmatic example of cooperation in cold atoms is the collective atomic recoil lasing (CARL) [6,7] observed when the atomic gas is illuminated with an intense far-off-resonance laser beam. The interaction mechanism between laser and atoms leads to an exponential growth of the probe light beam and to the formation of an atomic density grating with the optical wavelength periodicity. The atoms bunch in the wells of a pendulum potential formed by the interference between the counterpropagating pump and the probe fields, scattering photons coherently from the pump to the probe. CARL can operate in the “good-cavity regime” when the atoms are set in a ring cavity with negligible radiation losses, or in the “superradiant regime” when atoms are set in the free space or in a bad cavity. These regimes have been observed as superradiant Rayleigh scattering from a Bose-Einstein condensate (BEC) in free space [8–11] and recently with ultracold atoms in a high-finesse ring cavity [12–14]. CARL can operate also in a “quantum regime” [15–17] when the temperature of the atomic sample is below the recoil temperature and the gain bandwidth is less than the two-photon recoil frequency $\omega_r = \hbar q^2 / 2m$, where $q = |\vec{q}|$ and $\vec{q} = \vec{k}_s - \vec{k}$ is the difference between the scattered and incident wave vectors. In this case the recoil shifts the frequency of the scattered photon out of resonance, inhibiting further scattering processes. As a consequence the quantum CARL (QCARL) is characterized by a single-photon scattering with the collective momentum state of the cold sample changing by the two-photon recoil momentum $\hbar q$. As in the classical CARL, QCARL admits two different regimes depending on the value of the cavity linewidth κ : (a) the good-cavity regime, in which the atoms return to their initial momentum state after the emission of a 2π hyperbolic secant pulse; and (b) the superradiant regime, in which the

atoms move through adjacent recoil momentum states emitting each time a π hyperbolic secant pulse experiencing a sequence of superradiant processes interrupted only when the decoherence between momentum states prevails [8]. The emission frequencies in QCARL are discrete and determined by the difference between the final and the initial kinetic energies of each transition. In fact the atoms scatter the pump photons into the radiation mode, changing the momentum from the state $n=0, \pm 1, \dots$ [with momentum $p_z = n(\hbar q)$] to the state $n-1$, varying its kinetic energy by $E_{n-1} - E_n = \hbar\omega_r(1-2n)$. For each momentum transition between n and $n-1$ a coherent pulse is emitted, with frequency $\omega_s = \omega - \omega_r(1-2n)$, where ω is the pump frequency. Hence, the spacing between the emitted frequencies is $2\omega_r$. In the good-cavity quantum regime each atom initially at rest (i.e., in the state $n=0$) backscatters a single photon first from the pump to the cavity mode and afterward from the cavity mode to the pump, moving from the momentum state $n=0$ to $n=-1$ and back. On the contrary, in the superradiant quantum regime the atoms move through the negative recoil momentum states $n=-1, -2, \dots$ in a sequence of superradiant processes.

Both these processes can be enhanced if a term of frequency $\omega + \Delta$ (with $\Delta = 2\omega_r$) is added to the pump field of frequency ω . In this way, after the atoms have scattered the pump photon changing the momentum state from $n=0$ to -1 , they will also scatter the pump photon with frequency $\omega + \Delta$ further changing the momentum from $n=-1$ to -2 . The two scattered photons add coherently at the same frequency $\omega_s = \omega - \omega_r$. If the cavity linewidth κ is much smaller than the gain bandwidth (good-cavity regime), no other resonant scattering processes through other momentum transitions are possible and the two photons will be reabsorbed by the atoms which will return to the state $n=0$. In this way a closed three-momentum state system ($n=0, -1, -2$) is realized. In the superradiant regime with a two-frequency pump things change drastically also when the pump component at the frequency $\omega + \Delta$ is weak. The sequential superradiance is strongly accelerated, with the atoms rapidly moving through adjacent negative momentum states. The scattered field is an overlapping of many superradiant pulses, each one corresponding to a momentum transition $n \rightarrow n-1$. The radiation spectrum is composed by many lines separated by $2\omega_r$, downshifted with respect to the pump frequency ω .

In the following we analyze the effect of the two-frequency pump in the good-cavity and superradiant regimes

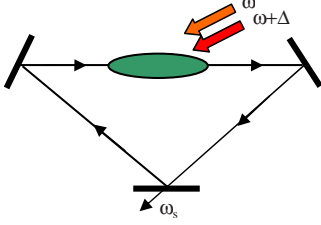


FIG. 1. (Color online) Schematic diagram illustrating the geometry of a two-frequency pump CARL experiment.

of QCARL for a BEC, neglecting nonideal behaviors, like decoherence and Doppler broadening, which will be considered in a more complete future analysis.

II. THE MODEL

The quantum collective atomic recoil laser with a two-frequency pump is described by the following equations for the order parameter $\Psi(z, t)$ of the matter field and the cavity mode field amplitude $a(t)$:

$$\frac{\partial \Psi}{\partial t} = \frac{i\hbar}{2m} \frac{\partial^2 \Psi}{\partial z^2} - g[\alpha^*(t) a e^{i(qz + \delta t)} - \text{c.c.}] \Psi, \quad (1)$$

$$\frac{da}{dt} = gN\alpha(t) \int dz |\Psi|^2 e^{-i(qz + \delta t)} - \kappa a, \quad (2)$$

where z is the coordinate along the cavity axis and $\alpha(t) = 1 + \epsilon \exp(-i\Delta t)$. These equations have been derived in the usual way [6, 15, 17] by performing the adiabatic elimination of the atomic internal degrees of freedom but replacing the pump field with $E_p = e^{i(\vec{k} \cdot \vec{x} - \omega t)} (E_0 + E_1 e^{-i\Delta t})$. In Eqs. (1) and (2) $a(t) = (\epsilon_0 V / 2\hbar \omega_s)^{1/2} E_s(t)$ is the dimensionless electric field amplitude of the scattered radiation beam with frequency ω_s , $g = (\Omega_0 / 2\Delta_0)(\omega \Delta^2 / 2\hbar \epsilon_0 V)^{1/2}$ is the coupling constant, $\Omega_0 = dE_0 / \hbar$ is the Rabi frequency of the pump laser incident with an angle ϕ with respect to the z axis ($\phi = \pi$ if counter-propagating), with electric field E_0 and frequency ω detuned from the atomic resonance frequency ω_0 by $\Delta_0 = \omega - \omega_0$. The pump laser has a frequency sideband of $\omega + \Delta$, with $\Delta = 2\omega_r$ [where $\omega_r = \hbar q^2 / 2m$ and $q = 2k \sin(\phi/2)$], and electric field E_1 , with $\epsilon = E_1 / E_0$. Since $\Delta \ll \omega$ and the condensate length L is much less than $2\pi c / \Delta$, we neglect the spatial modulation due to the difference of the two pump frequencies. The other parameters are $d = \hat{\epsilon} \cdot \vec{d}$, the electric dipole moment of the atom along the polarization direction $\hat{\epsilon}$ of the laser, V , the cavity mode volume, N , the total number of atoms in the condensate, $\delta = \omega - \omega_s$, and κ , the cavity linewidth. The emitted frequency value ω_s is within the cavity frequency linewidth, whereas the pump field is external to the cavity so that its frequencies are not dependent on those of the cavity. A sketch of a possible experimental configuration, similar to the one described in [14], is shown in Fig. 1.

The order parameter Ψ of the matter field is normalized such that $\int dz |\Psi|^2 = 1$. The second term in the right-hand side of Eq. (1) represents the self-consistent optical wave grating, whose amplitude depends on time according to Eq. (2). The

first term in the right-hand side of Eq. (2) represents the self-consistent matter-wave grating. Equations (1) and (2) have been written in the ‘‘mean-field’’ limit. Equation (2) describes approximately also the case of free space (see, for example, experiments described in [8–10]), modeling the radiation propagation by a damping term with $\kappa \approx c / 2L$, where L is the condensate length.

If the condensate is much longer than the radiation wavelength and approximately homogeneous, then periodic boundary conditions can be applied on the atomic sample and the order parameter can be written as $\Psi(z, t) = \sum_n c_n(t) u_n(z) e^{in\delta t}$, where $u_n(z) = (q/2\pi)^{1/2} \exp(inqz)$ are the momentum eigenstates with eigenvalues $p_z = n(\hbar q)$. Introducing the density matrix $\varrho_{m,n} = c_m c_n^*$ and $\omega_n = \omega_r n^2 + \delta n$, we obtain from Eqs. (1) and (2)

$$\begin{aligned} \frac{d\varrho_{m,n}}{dt} = & -i(\omega_m - \omega_n)\varrho_{m,n} + g[a\alpha^*(t)(\varrho_{m,n+1} - \varrho_{m-1,n}) \\ & + a^*\alpha(t)(\varrho_{m+1,n} - \varrho_{m,n-1})], \end{aligned} \quad (3)$$

$$\frac{da}{dt} = gN\alpha(t) \sum_n \varrho_{n,n-1} - \kappa a. \quad (4)$$

Before presenting the results of the numerical integration of Eqs. (3) and (4), it is worth investigating the equations obtained by reducing the Hilbert space to the one spanned by only the first three recoil momentum levels, $n=0, -1, -2$. Defining the three polarizations $B_1 = \varrho_{0,-1}$, $B_2 = \varrho_{-1,-2}$, $B_3 = \varrho_{0,-2}$ and the population differences $D_1 = P_0 - P_{-1}$ and $D_2 = P_{-1} - P_{-2}$, where $P_n = \varrho_{n,n}$, Eqs. (3) and (4) reduce to

$$\frac{dB_1}{dt} = -i(\delta - \omega_r)B_1 + g\alpha^*(t)aD_1 - g\alpha(t)a^*B_3, \quad (5)$$

$$\frac{dB_2}{dt} = -i(\delta - 3\omega_r)B_2 + g\alpha^*(t)aD_2 + g\alpha(t)a^*B_3, \quad (6)$$

$$\frac{dB_3}{dt} = -2i(\delta - 2\omega_r)B_3 + g\alpha^*(t)a(B_1 - B_2), \quad (7)$$

$$\frac{dD_1}{dt} = -g[\alpha^*(t)a(2B_1^* - B_2^*) + \text{c.c.}], \quad (8)$$

$$\frac{dD_2}{dt} = g[\alpha^*(t)a(B_1^* - 2B_2^*) + \text{c.c.}], \quad (9)$$

$$\frac{da}{dt} = gN\alpha(t)(B_1 + B_2) - \kappa a. \quad (10)$$

The presence of the pump sideband term at the frequency $\omega + \Delta$ will induce two sideband terms in the cavity field a which can be written in general as

$$a(t) = A_1(t) + A_2(t)e^{i\Delta t} + A_3(t)e^{-i\Delta t}, \quad (11)$$

where A_1 , A_2 , and A_3 are slowly varying functions. Furthermore, when $\delta = \omega_r$ the polarization B_1 is resonant, whereas B_2 and B_3 oscillate at the frequency $\Delta = 2\omega_r$. Hence, we can set

$B_{2,3} = \tilde{B}_{2,3} e^{i\Delta t}$, where $\tilde{B}_{2,3}$ are slowly varying functions. By substituting them, together with (11), in Eqs. (5)–(10) and neglecting the fast-oscillating terms proportional to $\exp(im\Delta t)$ with $m = \pm 1, \dots$ we obtain

$$\frac{dB_1}{dt} = -i\tilde{\delta}B_1 + g(A_1 + \epsilon A_2)D_1 - g(\epsilon A_1^* + A_2^*)\tilde{B}_3, \quad (12)$$

$$\frac{d\tilde{B}_2}{dt} = -i\tilde{\delta}\tilde{B}_2 + g(\epsilon A_1 + A_2)D_2 + g(A_1^* + \epsilon A_3^*)\tilde{B}_3, \quad (13)$$

$$\frac{d\tilde{B}_3}{dt} = -2i\tilde{\delta}\tilde{B}_3 + g(\epsilon A_1 + A_2)B_1 - g(A_1 + \epsilon A_3)\tilde{B}_2, \quad (14)$$

$$\frac{dD_1}{dt} = -g[2(A_1 + \epsilon A_3)B_1^* - (\epsilon A_1 + A_2)B_2^* + \text{c.c.}], \quad (15)$$

$$\frac{dD_2}{dt} = g[(A_1 + \epsilon A_3)B_1^* - 2(\epsilon A_1 + A_2)B_2^* + \text{c.c.}], \quad (16)$$

$$\frac{dA_1}{dt} = gN(B_1 + \epsilon\tilde{B}_2) - \kappa A_1, \quad (17)$$

$$\frac{dA_2}{dt} = gN\tilde{B}_2 - (\kappa + i\Delta)A_2, \quad (18)$$

$$\frac{dA_3}{dt} = \epsilon gNB_1 - (\kappa - i\Delta)A_3, \quad (19)$$

where $\tilde{\delta} = \delta - \omega_r$. Equations (12)–(19) describe the three-level dynamics of the collective atomic recoil lasing with a two-frequency pump.

III. THE GOOD-CAVITY QUANTUM REGIME

With a single-frequency pump the QCARL in the good-cavity regime is realized when $\kappa \ll g\sqrt{N} \leq 2\omega_r$ and $\delta = \omega_r$ [15]. In this regime only the first momentum recoil state $n = -1$ becomes occupied and the condensate behaves as a two-level system with only two momentum levels coupled with the radiation mode.

With a two-frequency pump no sidebands in the emitted field a will be generated, since the sideband fields A_2 and A_3 of Eq. (11) are out of resonance due to the detuning terms $\mp i\Delta A_{2,3}$ in Eqs. (18) and (19). The atoms scatter resonantly both the pump photons with frequencies ω and $\omega + \Delta$ into the same field A_1 with frequency $\omega_s = \omega - \omega_r$, undergoing two momentum transitions from $n=0$ to $n=-2$. In this case a pure three-level system, driven by two pump fields, is generated.

The good-cavity regime with a two-frequency pump is illustrated in Fig. 2 showing (a) the average number of photons emitted per atom, $|a|^2/N$, and (b) the populations of the three momentum levels, P_0 (dashed line), P_{-1} (continuous line), and P_{-2} (dotted line), vs t/τ [where $\tau = (g\sqrt{N})^{-1}$] obtained from the numerical integration of Eqs. (3) and (4) with

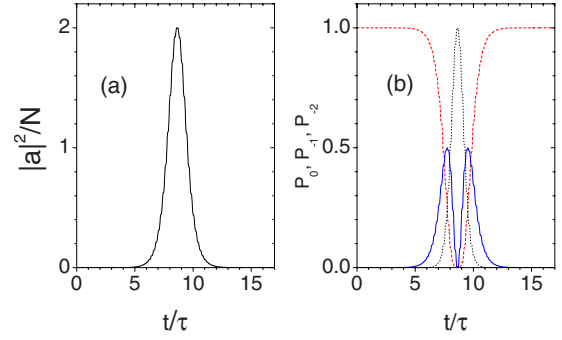


FIG. 2. (Color online) Good-cavity QCARL regime for $\kappa=0$, $g\sqrt{N}=0.063\omega_r$, $\epsilon=1$ and $\delta=\omega_r$. (a) $|a|^2/N$ and (b) populations of the three momentum levels, P_0 (dashed line), P_{-1} (continuous line), and P_{-2} (dotted line), vs t/τ , where $\tau = (g\sqrt{N})^{-1}$.

$\kappa=0$, $g\sqrt{N}=0.063\omega_r$, $\epsilon=1$ and $\delta=\omega_r$. The solution of the reduced Eqs. (12)–(19), with $A_2=A_3=0$, agrees perfectly with the exact solution demonstrating that in the good-cavity regime a single-frequency field $a=A_1$ is generated. As can be seen in Fig. 2(a), two photons with frequency $\omega_s = \omega - \omega_r$ are coherently emitted during the process transferring the atoms from $n=0$ to -2 and back.

IV. ACCELERATED SUPERRADIANCE

The QCARL superradiance with a single-frequency pump is realized for $\kappa \geq g\sqrt{N}$ and $G_{\text{SR}} \ll 2\omega_r$, where $G_{\text{SR}} = g^2N/\kappa$ is the superradiant gain [15,21]. The effect of a sideband at the frequency $\omega + \Delta$ in the pump is illustrated in Figs. 3 and 4, showing the results of the numerical integration for Eqs. (3) and (4) with $\kappa=20\omega_r$, $G_{\text{SR}}=0.2\omega_r$ and $\delta=\omega_r$. Figure 3(a) shows the average momentum in units of $\hbar q$, $\langle p \rangle = \sum_n n P_n$, vs t/τ_{SR} , where $\tau_{\text{SR}} = G_{\text{SR}}^{-1}$ is the superradiant time, for $\epsilon=0$ (dashed red line), 0.1 (continuous blue line) and 1 (dash-dotted black line). The sequential superradiance observed with the single-frequency pump is strongly accelerated when the sideband component is added to the pump. After the first

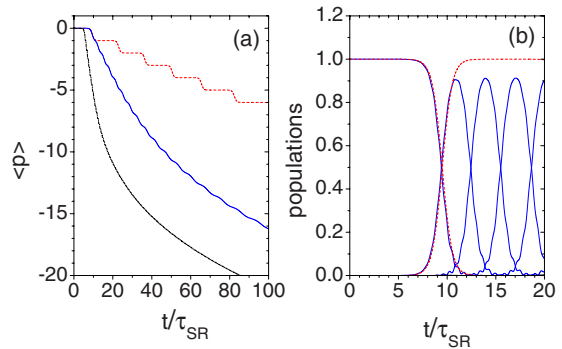


FIG. 3. (Color online) Superradiance (SR) and accelerated superradiance (ASR) for $\kappa=20\omega_r$ and $G_{\text{SR}}=0.2\omega_r$. (a) Average momentum $\langle p \rangle$ in units of $\hbar q$ vs t/τ_{SR} (where $\tau_{\text{SR}} = G_{\text{SR}}^{-1}$) for single-frequency pump, $\epsilon=0$ (dashed red line), and two-frequency pump with $\epsilon=0.1$ (continuous blue line) and 1 (dash-dotted black line). (b) Populations P_n vs t/τ_{SR} for $n=0, -1, \dots, -4$ with $\epsilon=0$ (dashed red line) and $\epsilon=0.1$ (continuous blue line).

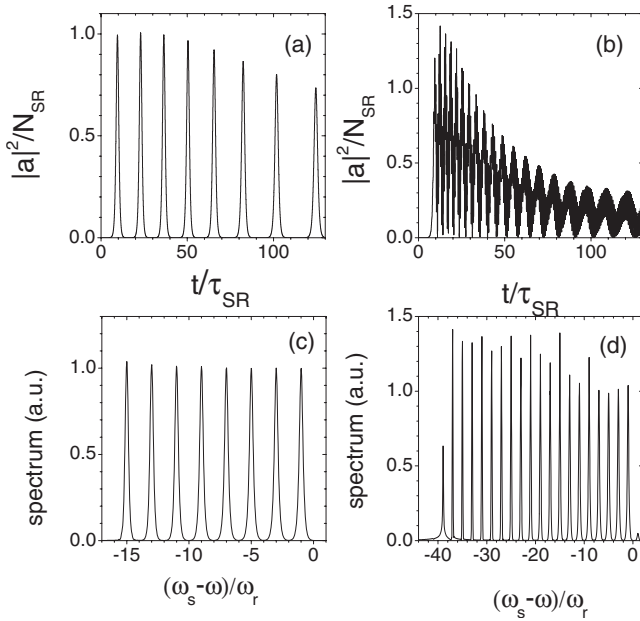


FIG. 4. Superradiance (SR) and accelerated superradiance (ASR). $|a|^2/N_{\text{SR}}$ vs t/τ_{SR} for (a) $\epsilon=0$ and (b) 0.1. Their respective spectra are shown in (c) and (d), vs $(\omega_s - \omega)/\omega_r$. The other parameters are the same as in Fig. 3.

momentum transition atoms move through the recoil momentum levels in a rapid sequence of superradiance transitions down to large and negative momentum states, as shown in Fig. 3(b) where the populations P_n of the first levels (up to $n=-4$) are plotted for $\epsilon=0$ (dashed red line) and 0.1 (continuous blue line).

The scattered intensity $|a|^2/N_{\text{SR}}$ [expressed as the average photon number relative to the maximum superradiant value $N_{\text{SR}}=(gN/2\kappa)^2$] is shown in Fig. 4 for (a) $\epsilon=0$ and (b) 0.1. The corresponding spectra after $t=130\tau_{\text{SR}}$ are shown in Figs. 4(c) and 4(d), respectively, as a function of $(\omega_s - \omega)/\omega_r$. For each momentum transition between n and $n-1$ a superradiant pulse is emitted with frequency $\omega_s = \omega - (1-2n)\omega_r$, and $n=0, -1, \dots$. Whereas for the single-frequency pump ($\epsilon=0$) superradiance generates a sequence of well-separated pulses, the pump sideband enhances the superradiant cascade accelerating the atoms to a large and negative momentum state, emitting a sequence of closely spaced SR pulses with a discrete spectrum composed by narrow lines separated by $2\omega_r$. In the good-cavity regime a single-frequency field at $\omega_s = \omega - \omega_r$ (resonant with both the first two momentum transitions driven by the two pump frequencies) is generated while in the superradiant regime two sidebands at $\omega_s = \omega - \omega_r \pm \Delta$ are generated during the two first transitions, as can be seen by solving the reduced three-level model of Eqs. (12)–(19). In this case the sideband at frequency $\omega_s = \omega - 3\omega_r$ will combine

with the pump sideband at $\omega + 2\omega_r$ stimulating the transition from $n=-2$ to -3 with frequency difference $5\omega_r$. The process will continue indefinitely until the decoherence prevails and the coherences between the momentum levels decay to zero. We must also note that the present model does not properly take into account the real transmission curve of the cavity, in which any frequency out of the cavity linewidth does not oscillate: in a real experiment with a high-finesse cavity the maximum number of generated sidebands will be only of the order of $\kappa/2\omega_r$. Furthermore, superradiance has been observed also without a cavity, with the radiation emitted along the end-fire modes of an elongated condensate [8–11]. The model here considered describes as well these experiments [18] if a very large effective linewidth $\kappa \sim c/2L$ is assumed, where L is the condensate length. In this kind of experiment it seems relatively easy to observe the accelerated superradiance just by adding a sideband to the pump field.

V. CONCLUSIONS

In conclusion, we have demonstrated that a bichromatic pump with frequency separation $\Delta=2\omega_r$ allows for the observation of different regimes in the quantum collective atomic recoil laser. In the good-cavity regime, when the cavity linewidth is much smaller than the gain bandwidth, the BEC behaves as a three-level system, with each atom emitting two equal-frequency coherent photons. Eventually, with addition of relaxation terms to the polarization equations (12)–(14), the model describes typical behaviors well known in three-level systems as, for instance, electromagnetic-induced transparency or population trapping [19]. So QCARL with a two-frequency pump, using a BEC in a high-finesse ring cavity, could be conveniently implemented for typical applications expected from coherent three-level systems such as, for instance, for creating entangled states or for storing and transferring codified information between radiation and cold matter [20,22].

In the superradiant regime the addition of a weak term with frequency $\omega + \Delta$ to the pump will strongly enhance the collective process, accelerating the superradiant cascade through adjacent recoil momentum levels and emitting a train of pulses with equally spaced frequencies separated by Δ . We note that an experiment with a bichromatic pump in the superradiant Rayleigh scattering has been recently performed in a different configuration [23] enhancing the backward emission in which the atoms reabsorb a photon from the superradiant radiation and emit a stimulated photon into the pump laser, recoiling oppositely to the pump. Instead, in our case the pump field at the frequency $\omega + \Delta$ induces further recoil in the pump direction, accelerating the atoms toward large-momentum states without inducing any velocity spread in the atomic sample.

- [1] F. Brennecke, T. Donner, S. Ritten, M. Köhl, and T. Esslinger, *Nature (London)* **450**, 268 (2007).
- [2] Y. Colombe, T. Steinmetz, G. Dubois, F. Linke, D. Hunger, and J. Reichel, *Nature (London)* **450**, 272 (2007).
- [3] J. M. Zhang, W. M. Liu, and D. L. Zhou, *Phys. Rev. A* **77**, 033620 (2008).
- [4] An-Chun Ji, X. C. Xie, and W. M. Liu, *Phys. Rev. Lett.* **99**, 183602 (2007).
- [5] S. Slama, S. Bux, G. Krenz, C. Zimmermann, and Ph. W. Courteille, *Phys. Rev. Lett.* **98**, 053603 (2007).
- [6] R. Bonifacio and L. De Salvo Souza, *Nucl. Instrum. Methods Phys. Res. A* **341**, 360 (1994).
- [7] R. Bonifacio, L. De Salvo, L. M. Narducci, and E. J. D'Angelo, *Phys. Rev. A* **50**, 1716 (1994).
- [8] S. Inouye, A. P. Chikkatur, D. M. Stamper-Kurn, J. Stenger, D. E. Pritchard, and W. Ketterle, *Science* **285**, 571 (1999).
- [9] S. Inouye, T. Pfau, S. Gupta, A. P. Chikkatur, A. Görlitz, D. E. Pritchard, and W. Ketterle, *Nature (London)* **402**, 641 (1999).
- [10] M. Kozuma, Y. Suzuki, Y. Torii, T. Sugiura, T. Kugam, E. W. Hagley, and L. Deng, *Science* **286**, 2309 (1999).
- [11] L. Fallani, C. Fort, N. Piovella, M. M. Cola, F. S. Cataliotti, M. Inguscio, and R. Bonifacio, *Phys. Rev. A* **71**, 033612 (2005).
- [12] D. Kruse, C. von Cube, C. Zimmermann, and P. W. Courteille, *Phys. Rev. Lett.* **91**, 183601 (2003).
- [13] C. von Cube, S. Slama, D. Kruse, C. Zimmermann, P. W. Courteille, G. R. M. Robb, N. Piovella, and R. Bonifacio, *Phys. Rev. Lett.* **93**, 083601 (2004).
- [14] S. Slama, G. Krenz, S. Bux, C. Zimmermann, and P. W. Courteille, *Phys. Rev. A* **75**, 063620 (2007).
- [15] N. Piovella, M. Gatelli, and R. Bonifacio, *Opt. Commun.* **194**, 167 (2001).
- [16] M. G. Moore, O. Zobay, and P. Meystre, *Phys. Rev. A* **60**, 1491 (1999).
- [17] N. Piovella, M. M. Cola, and R. Bonifacio, *Phys. Rev. A* **67**, 013817 (2003).
- [18] N. Piovella, M. Gatelli, L. Martinucci, R. Bonifacio, B. W. J. McNeil, and G. R. M. Robb, *Laser Phys.* **12**, 188 (2002).
- [19] S. E. Harris, *Phys. Today* **50**(7), 36 (1997).
- [20] D. F. Phillips, A. Fleischhauer, A. Mair, R. L. Walsworth, and M. D. Lukin, *Phys. Rev. Lett.* **86**, 783 (2001).
- [21] G. R. M. Robb, N. Piovella, and R. Bonifacio, *J. Opt. B: Quantum Semiclassical Opt.* **7**, 93 (2005).
- [22] C. Liu, Z. Dutton, C. H. Behroozi, and L. V. Hau, *Nature (London)* **409**, 490 (2001).
- [23] N. Bar-Gill, E. E. Rowen, and N. Davidson, *Phys. Rev. A* **76**, 043603 (2007).